The influence of port shape on gas pulsations in a screw compressor discharge chamber

E.Mujic, A.Kovacevic, N.Stosic, I.K.Smith
City University London
Centre for Positive Displacement Compressor Technology
City University, London EC1V OHB, U.K.

ABSTRACT

Gas pulsations in suction and discharge chambers are widely accepted to be a significant source of noise in screw compressors. This paper analyses the influence of both the compressor operating conditions and its geometric characteristics on the level of gas pulsations generated in its discharge chamber. The transfer function of the discharge port area is identified here as an important parameter influencing gas pulsations. It is shown how the gas pulsation amplitude in the discharge chamber can be reduced by optimization of its port shape.

NOMENCLATURE

A	area
dA_i	finite small area of the discharge port
φ	angular coordinate in cylindrical coordinate system
$\varphi_{i1}, \varphi_{i2}$	lower and upper boundary for finite small area
h_{in}	specific enthalpy flow in chamber
h_{out}	specific enthalpy flow from chamber
i	arbitrary position of the finite small area
m	fluid mass in chamber
$\dot{m}_{in}$	mass flow in chamber

$\dot{m}_{out}$	mass flow from chamber
n	number of finite divisions of the discharge port
p	fluid pressure in chamber
$\dot{Q}$	heat transfer between fluid and chamber surrounding
R	radial coordinate in cylindrical coordinate system
R_i, R_{i+1}	lower and upper boundary for finite small area
$R_{\max}, R_{\min}$	maximum and minimum radius of axial discharge port
ρ	fluid density
t	time
U	internal energy
v	fluid velocity
V	fluid volume in chamber
z	coordinate Z in cylindrical coordinate system
z_i, z_{i+1}	lower and upper boundary for finite small area

Subscripts

A	axial discharge port	M	male side of the discharge port
dc	discharge chamber	out	discharge chamber outlet
dp	discharge port	R	radial discharge port
F	female side of the discharge port	wc	working chamber

1. INTRODUCTION

The suction and discharge chambers of a screw compressor are connected to the working chambers only periodically. This creates unsteady flow, variation of mass and hence pressure pulsations in them during both the suction and discharge processes through the compressor ports. These create both vibration and noise. The amplitude of the gas pulsations in the compressor discharge chamber is much higher then those in the suction chamber. Therefore many authors consider the gas pulsations in a screw compressor discharge chamber to be the main source of noise.

Intensive research on gas pulsations in screw compressors started in 1986 when *Fujiwara and Sakurai* [2] first measured gas pulsation, vibration, and noise in a screw compressor. After that *Koai and Soedel* [5,6] 1990, developed an acoustic model in which they theoretically analyzed the flow pulsation in a twin screw compressor and investigated how it was related to compressor performance. More recently *Sangfors* [9] in 1999, *Tanttari* 2000 [11] and *Huagen et al* 2004 [4] developed mathematical models for the prediction of gas pulsations in screw compressor suction and discharge chambers.

All these authors explored the influence of various screw compressor working and design parameters upon gas pulsations in the compressor suction and discharge chambers. Some authors, such as *Koai and Soedel* [5] recognized the influence of the compressor port area and recommended that the effect of the port shape on noise be further investigated. *Mujic et al* 2005 [8] reported that changing the shape of a screw compressor discharge port leads to different gas pulsation levels in the discharge chamber. Reduction of pulsation amplitude leads to lower overall levels of compressor noise. This led to further investigation of this effect.

2. PARAMETERS WHICH INFLUENCE GAS PULSATIONS

In order to reduce level of gas pulsations in the discharge chamber parameters which influence gas pulsations have to be determined. Previous studies have reported some working and design parameters. Their influence upon gas pulsations also has been examined. However, there was no explanation why these parameters have been selected among many others. To investigate this and to find is there any other not mentioned influential parameter the analysis of the discharge process has to be carried out. So, in text as follows main influential parameters will be determined and possibility to use them as an optimisation parameter will be discussed.

2.1. Main factors affecting gas pulsations

Analysis of the discharge process in screw compressor has to be performed to identify factors which influence level of gas pulsations. So, in Figure 1 are presented working and discharge chambers connected together through discharge port. Both of considered chambers are also connected to the rest of the system. The working chamber is connected to other working chambers or suction through the leakage paths, while the discharge chamber is connected to the discharge pipe. These connections between the chambers and their surrounding always present. However, connection between chambers themselves is of periodical nature. Accordingly, the discharge process of one working chamber starts with opening of the discharge port and lasts until the port is closed.

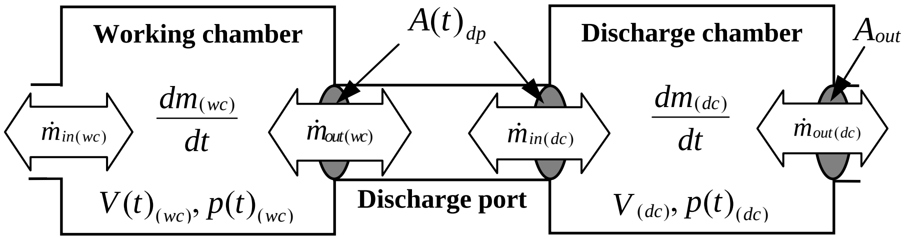

Figure 1 Screw compressor discharge system

Let's consider gas conditions in both chambers during the cycle. If heat transfer through chamber walls is neglected then gas condition in chambers are determined by change in chamber volume and mass and energy transfer rate between chamber and surrounding. Working chamber volume is defined by volume transfer function $V(t)_{(wc)}$ which determines gas condition in the chamber. However, volume of the discharge chamber $V_{(dc)}$ does not influence gas condition in this chamber because it is constant. Therefore, it remains that gas condition in the discharge chamber are influenced only by mass and energy transfer. As heat transfer through walls can be neglected the only way to transfer energy is through mass flow. So, only mass flows to and from discharge chamber affects gas conditions in it. This is in line with definitions of gas pulsations in a chamber which states that these occur if mass is added in a chamber at an unstable rate.

Presented in Figure 1 are two mass flows between the discharge chamber and its surrounding. The first is mass inflow to the discharge chamber from the compressor working chamber. The second one is mass outflow from the discharge chamber into compressor discharge system consisting of pipes, oil separators etc. Both flows being time dependant need to satisfy continuity equations (1) and (2).

$$\dot{m}_{in(dc)} = \rho v A(t)_{dp} \tag{1}$$

$$\dot{m}_{out(dc)} = \rho v A_{out} \tag{2}$$

Equations (1) and (2), show that both mass flows depend on the instant gas density and the velocity. The fluid velocity depends on difference of fluid enthalpies in chambers. Or expressed for compressors in more appropriate way, the velocity depends on pressure difference between chambers. The gas density is also parameter which is related to the chamber pressures. Therefore, the pressure difference between working and discharge chamber is parameter which influences level of gas pulsations. Pressure difference between discharge chamber and pipe is rather consequence of the gas pulsations then their cause.

Analyzing equations (1) and (2) two more parameters which influence mass flows and later gas pulsations can be recognized. The first one is the outlet area A_{out} where the discharge chamber is connected to the discharge pipe. The size of the outlet is constant and it is good to make it as large as possible. A larger area will cause lower pressure difference for the same flow between discharge chamber and pipe. That will stabilize pressure in the discharge chamber.

Another parameter which influences mass flow and has been neglected in previous studies is cross sectional area between working and discharge chamber $A(t)_{dp}$, defined as discharge port. According to equation (1)the effect of changing the size of the discharge port is of the same order of magnitude as those of changes in density or velocity. This implies that the gas flows and pressure variations can be altered by modifying the transfer function of the discharge port area. This can be achieved by changing the shape of the discharge port. The influence of different discharge ports has been noticed but not explained in papers published by *Errol & Ahmet* [1] and *Mujic et al*. [8]. Difference in noise, identified trough their research, can be explained only by the different cross sectional area of the ports. As far as author is concerned there are no published records on any investigation of this phenomenon.

So, two basic influential parameters which influence level of gas pulsations in the discharge chamber are identified as pressure difference and transfer function of the discharge port area. In order to decrease amplitude of gas pulsations in the discharge chamber these two parameters needs to be optimised. It has to be explored is it necessary to optimise both of these two parameters or only one of them.

Pressure difference has been explored in many studies. Maybe the most relevant are studies from *Koai & Soedel* and *Sangfors*. They recognise pressure difference as a cause for gas pulsations and they have explored influence of many operational or design parameters upon gas pulsations. Influence of these parameters upon as pulsations is presented as follows.

2.2. Working conditions

Discharge pressure is on parameter which determines pressure difference between working and discharge chamber when discharge starts. That pressure difference is lowest when the discharge pressure is equal to the pressure in the working chamber. This has been reported by *Koai* and *Soedel* [5]. They noticed that the gas pulsations as function of the discharge pressure have a minimum. This is also confirmed later by *Sangfors* [9]. According to *Huagen et al* [4], this minimum corresponds to the discharge pressure that matches the machine built-in volume ratio. *Koai and Soedel* [5] claim that this minimum does not correspond exactly to that pressure, while *Gavric* [3] consider that it coincides with the small undercompression.

Compressor speed. S*angfors* [9] and *Huagen* [4] concluded that the amplitude of the pressure pulsations during the discharge process increases with the rotational speed.
Oil influence. Oil has an attenuating influence upon the noise generation process. According to *Sangfors* [9] this is significant at harmonics higher than the 3rd order but *Tanttari* [11] states that this is noticeable only above the 5th order.

2.3. Compressor design parameters

Compressor clearances. Reduction of leakage within the compressor, caused by smaller clearances, increases the noise generated in the discharge port. *Soedel* [5] and *Sangfors* [9] reported that for the same working conditions, changed compressor clearances result in a change in the working chamber pressure and fluid flow through the discharge port.

Discharge chamber length. According to *Sangfors* [9] the gas pulsations and generated SPL are affected by the discharge chamber length. This influence is significant and the sound pressure level expressed as a function of chamber length also has a minimum.

Number of rotor lobes. According to *Sangfors* [9], the number of rotor lobes influences the noise level. Rotors consisting of more lobes generally generate a lower sound pressure level in operation then those with fewer lobes.

All these parameters have one common thing which is directly influence on pressure difference between working and discharge chamber. Operational parameters such discharge pressure and compressor speed have high influence on gas pulsations. However, those parameters depends of purpose for which compressor is in use. It makes them inappropriate for optimisation. Compressor design parameters as built in volume ratio, clearances, number of lobes, sealing line etc. also affects gas pulsations. But trying to decrease gas pulsations by optimising any of these parameters degrades compressor performances which has been confirmed by experiment. This makes the set of compressor design parameters also inappropriate for optimisation. This means that decrease in gas pulsations in the compressor discharge chamber can not be achieved by changing pressure difference.

There are no records which will explain how shape of the discharge ports affects gas pulsations in screw compressor. The influence of different discharge ports has been noticed but not explained in papers published by *Errol & Ahmet* [1] and *Mujic et al*. [8]. Therefore this behaviour should be explored and if possible employed in reduction of compressor noise. To explore influence of the discharge port area upon gas pulsations it is necessary to avoid any change in pressure difference. So, the other design parameters such built in volume ratio, clearances, sealing line etc. should stay unchanged. This will also reduce degradation of compressor performances. To evaluate influence of the area transfer function the mathematical model of the compressor discharge process will be used.

3. MATHEMATICAL MODELLING OF THE DISCHARGE FLOW PROCESS

The mathematical model of screw compressor discharge process is based on a model described by *Stosic and Hanjalic* [10]. That mathematical model consists of set of differential equations for mass and energy conservation in a control volume which can be suction, working or discharge chamber. This system of equations is enclosed by set of algebraic equations which describe various phenomena inside of screw compressor such as suction or discharge flow, fluid injection, heat transfer. The relation between fluid properties is established through the equation of state for either ideal gas or real fluids. Internal energy, rather than enthalpy, is used as the derived variable to reduce calculation time. Computation is then carried out through a series of iterative cycles until the solution converges. Pressure transfer function can then be derived directly from it, together with the remaining required thermodynamic properties.

The model which will be described here is simplified model of that used by *Stosic and Hanjalic* [10]. The model will describe only screw compressor discharge process. Therefore, system consists of two control volumes, working and discharge chamber, as it is shown in Figure 1. Neglected here are also, flow through compressor clearances, fluid injection and heat transfer. Ideal gas has been used as a working fluid. These simplification although affect accuracy of predicted results, will not affect influence of the discharge port shape upon gas pulsations if it exists.

3.1. Mass conservation law

For thermodynamic system shown in Figure 1 the equations of mass conservation for the working chamber (3) and discharge chamber (4) are:

$$\frac{dm_{(wc)}}{dt} = \dot{m}_{in(wc)} - \dot{m}_{out(wc)} \tag{3}$$

$$\frac{dm_{(dc)}}{dt} = \dot{m}_{in(dc)} - \dot{m}_{out(dc)} \tag{4}$$

It can be seen from Figure 2, that when one working chamber starts its discharge the previous chamber has still not finished. Also, before the discharge of one chamber ends, the discharge of the next chamber starts. This affects the mass and energy inflow into discharge chamber. So, the mass inflow into the discharge chamber consists of flows from more then one working chambers. Due to that equation for the mass inflow into discharge chamber takes into account outflows from *n* working chambers:

$$\dot{m}_{in(dc)} = \sum_{i=1}^{n} \dot{m}_{out(wc)i} \tag{5}$$

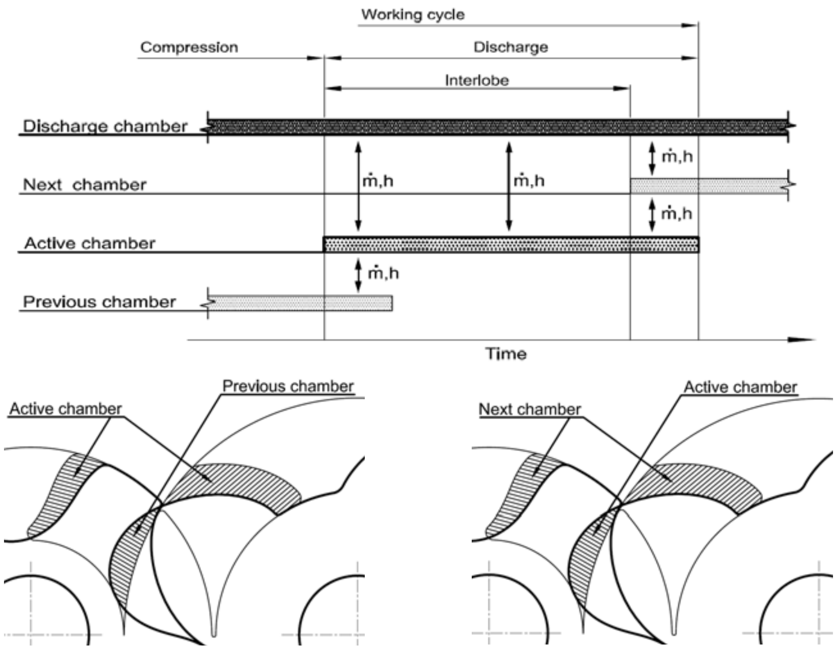

Figure 2 Screw compressor discharge process

Each of the mass flow rates in the above equation satisfies the continuity equation. As an example presented here is mass outflow from the working chamber:

$$\dot{m}_{out(wc)i} = \left(\rho v A\right)_{(wc)i} \tag{6}$$

Fluid velocity v between working and discharge chamber is calculated by equation:

$$v = \mu\sqrt{2(h_{wc} - h_{dc})} \tag{7}$$

where the upstream enthalpy is h_{wc} while downstream enthalpy is h_{dc}. In case that upstream enthalpy in the discharge chamber is higher then enthalpy in working chamber the reverse flow occurs. Accordingly to it the fluid density ρ is determined by higher enthalpy value. The area A is the cross sectional area of the discharge port connected to the working chamber *i*. This area is of complex shape and changes in time. Since the accuracy of the simulation depends on the size and gradient of that area, it is necessary to avoid any approximation and to accurately calculate the size of the discharge port area for any arbitrary rotor position and any shape of the discharge port and rotor profiles. Also to analyze the influence of different shapes of discharge ports on gas pulsations, it is necessary to quantify their difference in the model. This can be done providing the model with the actual size of the discharge port area of different ports. Numerical method for obtaining transfer function of the discharge port area will be presented later.

3.2. Energy conservation law

The equations for conservation of internal energy for compressor are given for the working chamber (8) and the discharge chamber (9) as follows:

$$\frac{dU_{(wc)}}{dt} = \dot{m}_{in(wc)} h_{in(wc)} - \dot{m}_{out(wc)} h_{out(wc)} + \dot{Q} - \left(p \frac{dV}{dt} \right)_{(wc)} \tag{8}$$

$$\frac{dU_{(dc)}}{dt} = \dot{m}_{in(dc)} h_{in(dc)} - \dot{m}_{out(dc)} h_{out(dc)} + \dot{Q} \tag{9}$$

Here enthalpy inflow into discharge chamber also consists of outflows from the *n* working chambers which are connected to discharge chamber at the same time:

$$\dot{m}_{in(dc)} h_{in(dc)} = \sum_{i=1}^{n} \dot{m}_{out(wc)i} \cdot h_{out(wc)i} \tag{10}$$

3.3. Starting and boundary conditions

Starting conditions for model explained in [10] are usually boundary conditions applied on compressor suction. However, the model employed here does not have suction and compression part of the compressor cycle. Therefore this model requires starting conditions to be provided when discharge starts. These are gas temperature and pressure at the compression end. For gas temperature the temperature of gas in outlet reservoir can be used. Gas pressure can be obtained from equation (11) if adiabatic compression is assumed:

$$p_{ce} = p_{cs} \left(\frac{V_{cs}}{V_{ce}} \right)^{\chi} \tag{11}$$

Outlet boundary conditions in 1-D model are presented by gas pressure and temperature in outlet reservoir. Outlet reservoir is enclosed and gas conditions are influenced much by pressure variations in the discharge chamber. It would be wrong to assume constant pressure in the outlet reservoir. Pressure variations in the outlet reservoir can be calculated by equation 3.15 [9].

$$p_d(t) = \frac{\rho c}{A} \left(\dot{V}(t) - \dot{V}_{av} \right) \tag{12}$$

This assumes discharge pipe of the infinite length. This excludes possibility of the wave reflection from the discharge system. This means that only influence of the incident wave created in discharge port will be accounted.

3.4. Transfer function of the discharge port area

In order to satisfy these requirements a numerical integration method has been developed. The calculation method described in here is one of the possible approaches which can be employed in order to obtain accurate values of the discharge port area for any shape of the compressor discharge port and for any profile of the compressor rotors.

The axial, male and female parts of the discharge port have four separated curves which defines the port shape Figure 3.a. Two of them C_1 and C_2, are arches which are usually of the same size as rotor outer and inner diameter. The third curve C_3 is on the outer side of the port is usually defined by the rotor profile, but it is can be any other shape. The curve C_4 is defined by the shape of the sealing line. Curves C_3 and C_4 are usually given as a set of points in the Cartesian coordinate system. To calculate the discharge port area it is easier to transfer these curves into cylindrical coordinate system.

$$\mathrm{C}_3(x, y) = \mathrm{C}_3(r, \varphi) \tag{13}$$

$$\mathrm{C}_4(x, y) = \mathrm{C}_4(r, \varphi) \tag{14}$$

The pure transformation from one to another coordinate system would not make any benefit. The curves C_3 and C_4 very often do not have the same number of the control points. The transformation should describe these two curves by the same number of the control points and to position each two associated points on these two curves on the same radius. In order to do that the uniform distribution of the radii has been made between $R_{M1}(R_{F1})$ and $R_{M2}(R_{F2})$. The section points between arches defined by these radii and curves C_3 and C_4 are two new sets of control points which very accurate describe curves C_3 and C_4 as shown in Figure 3.b.

Now it is possible to define finite number of small areas ΔA_{MAi} on male port side which are positioned between two nearest radii r_{MAi} and r_{MAi+1} and port boundaries as shown in Figure 3.d. Port boundaries depend of the position of both rotors and they can be different for any of the observed areas as shown on Figure 3.c. To employ the same logic it is necessary to transform the rotor profile in the same manner as it has been done for the discharge port curves. By this method any small area ΔA_{MAi} of the male side of the discharge port lays between two arches of the known radii which starts at known angle $\varphi_{1MAi}(\varphi_{1FAi})$ and finishes at also known angle $\varphi_{2MAi}(\varphi_{2FAi})$. The same principle applies for the female port side. The simplest case, when the observed area lay between rotor trailing edge and opening curves of the discharge port, is shown on the Figure 3.d.

The equations (15) and (16) calculate the value of the observed small the discharge port area on male and female side.

$$\Delta A_{MAi} = \int_{r_{MAi}}^{r_{MAi+1}} dr \int_{\varphi_{1MAi}}^{\varphi_{2MAi}} r_{MAi} \cdot d\varphi \qquad (15)$$

$$\Delta A_{FAi} = \int_{r_{FAi}}^{r_{FAi+1}} dr \int_{\varphi_{1FAi}}^{\varphi_{2FAi}} r_{FAi} \cdot d\varphi \qquad (16)$$

The whole area of the axial discharge port on male and female side can be calculated by adding all small areas together:

$$A_{MA} = \sum_{i=1}^{n_M} A_{MAi} \qquad (17)$$

$$A_{FA} = \sum_{i=1}^{n_F} A_{FAi} \qquad (18)$$

The whole area of the axial discharge port is then:

$$A_A = \sum_{i=1}^{n_M} \left(\int_{r_{MAi}}^{r_{MAi+1}} dr \int_{\varphi_{1MAi}}^{\varphi_{2MAi}} r_{MAi} \cdot d\varphi \right) + \sum_{i=1}^{n_F} \left(\int_{r_{FAi}}^{r_{FAi+1}} dr \int_{\varphi_{1FAi}}^{\varphi_{2FAi}} r_{FAi} \cdot d\varphi \right) \qquad (19)$$

The radial, male and female parts of the discharge port are enclosed by 3 curves. Curves C_1 are arches on the discharge end plane defined by male and female rotor radius. Curve C_2 is casp line while opening port curves C_3 are male and female helix as shown on Figure 3.e. Helix control points are all on the same radius in a cylindrical coordinate system. In this case the φ and z coordinates are variable. Taking these changes into account the same method which has been used for the calculation of the axial discharge port can be employed again. The Figure 3.f shows the basic principle of the area calculation of the radial discharge port. Here is recognised small area ΔA_{FRi} of the female side of discharge port is lays between two arches of the known positions z_{FRi} and z_{FRi+1} which start at known angle $\varphi_{1FRi}(\varphi_{1MRi})$ and finishes at also known angle $\varphi_{2FRi}(\varphi_{2MRi})$. Taking into account variable boundaries of the port it is possible to calculate value of the finite small area on male and female port side by equations (20) and (21).

$$\Delta A_{MRi} = \int_{z_{MRi}}^{z_{MRi+1}} dz \int_{\varphi_{1MRi}}^{\varphi_{2MRi}} r_M \cdot d\varphi \qquad (20)$$

$$\Delta A_{FRi} = \int_{z_{FRi}}^{z_{FRi+1}} dz \int_{\varphi_{1FRi}}^{\varphi_{2FRi}} r_F \cdot d\varphi \qquad (21)$$

The whole area of the radial discharge port on male and female side can be calculated by adding all small areas together as shown in equations (22) and (23):

$$A_{MR}=\sum_{i=1}^{n_M}\Delta A_{MRi} \tag{22}$$

$$A_{FR}=\sum_{i=1}^{n_F}\Delta A_{FRi} \tag{23}$$

The whole area of the radial discharge port is then calculated by equation (24):

$$A_R=\sum_{i=1}^{n_{MR}}\left(\int_{z_{MRi}}^{z_{MRi+1}}dz\int_{\varphi_{1MRi}}^{\varphi_{2MRi}}r_M\cdot d\varphi\right)+\sum_{i=1}^{n_{FR}}\left(\int_{z_{FRi}}^{z_{FRi+1}}dz\int_{\varphi_{1FRi}}^{\varphi_{2FRi}}r_F\cdot d\varphi\right) \tag{24}$$

The size of the discharge port for any arbitrary rotor position is calculated as:

$$\begin{aligned}A_R=&\sum_{i=1}^{n_M}\left(\int_{r_{MAi}}^{r_{MAi+1}}dr\int_{\varphi_{1MAi}}^{\varphi_{2MAi}}r_{MAi}\cdot d\varphi\right)+\sum_{i=1}^{n_F}\left(\int_{r_{FAi}}^{r_{FAi+1}}dr\int_{\varphi_{1FAi}}^{\varphi_{2FAi}}r_{FAi}\cdot d\varphi\right)\\&+\sum_{i=1}^{n_{MR}}\left(\int_{z_{MRi}}^{z_{MRi+1}}dz\int_{\varphi_{1MRi}}^{\varphi_{2MRi}}r_M\cdot d\varphi\right)+\sum_{i=1}^{n_{FR}}\left(\int_{z_{FRi}}^{z_{FRi+1}}dz\int_{\varphi_{1FRi}}^{\varphi_{2FRi}}r_F\cdot d\varphi\right)\end{aligned} \tag{25}$$

The equation (25) calculates area of the discharge port exposed to the working chamber for arbitrary rotor position determined by rotation angle θ of the male rotor. All angles on male and female side for axial and radial part of the port are in function of rotation angle of male rotor as shown in equations (26) and (27).

$$\varphi_{MA}=\varphi_{MR}=\theta \tag{26}$$

$$\varphi_{FA}=\varphi_{FR}=\theta\frac{z_1}{z_2} \tag{27}$$

Transfer function of the discharge port area is obtained by use of equation (25) for many different position of the male rotor during one working cycle. The largest part of the working cycle the discharge port is closed if one working chamber is considered which makes that discharge port area is equal to zero. Figure 3.g shows the area transfer function during the discharge process.

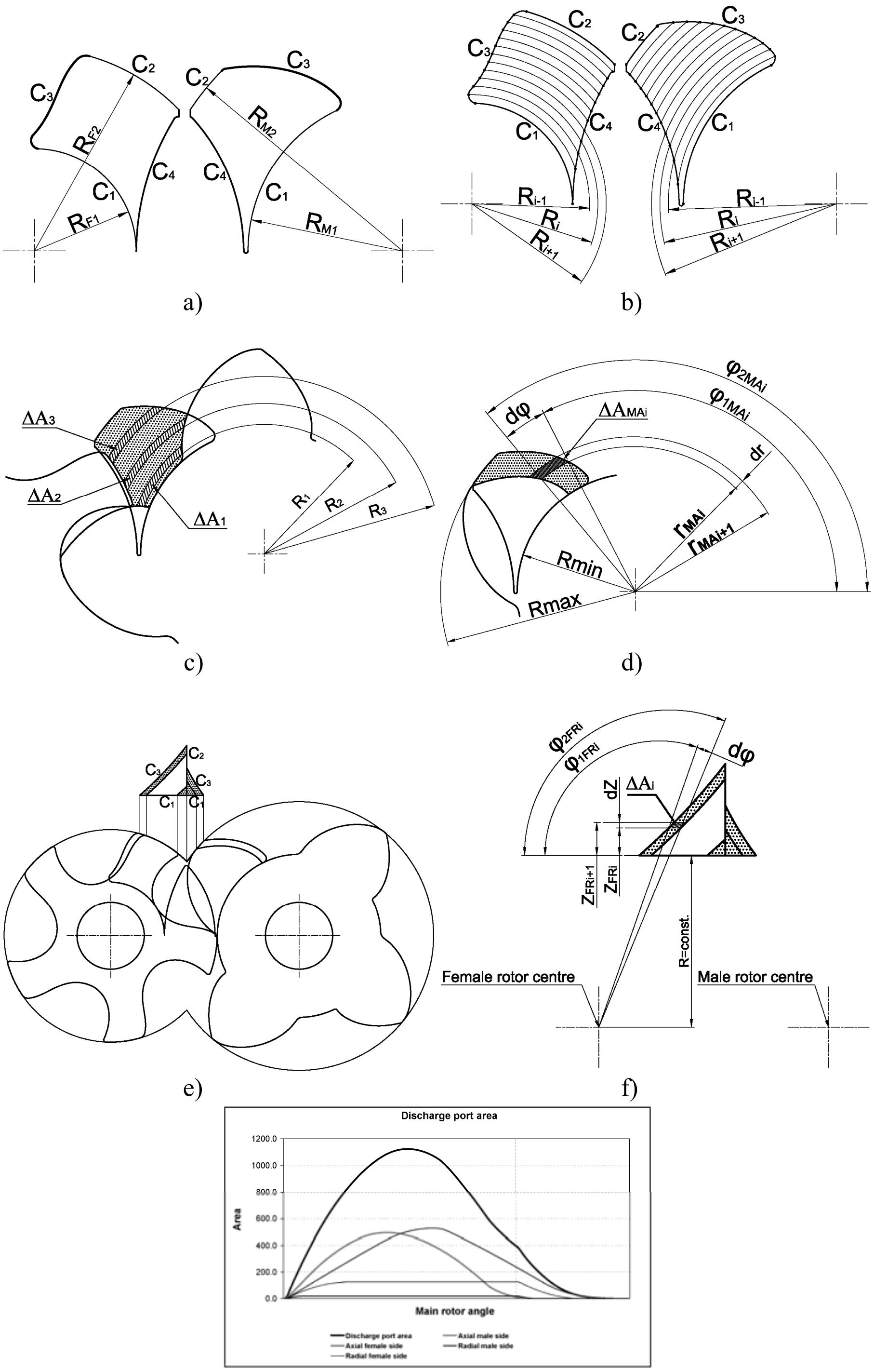

Figure 3 Principle of the discharge port area calculation

4. APPLICATION

Numerical and experimental methods were employed to investigate influence of the discharge port shape upon level of gas pulsations. Pressure transfer functions in the discharge chamber fro two different shapes of the discharge port are predicted by use of the developed thermodynamic model. Predicted results are later validated by experiment.

4.1. Compressor testing range and instrumentation

For investigation purpose an oil flooded air screw compressor has been used here. The most important compressor parameters are given in Table 1. Oil flooded compressor is used due to its operation over larger pressure range which develops higher gas pulsations comparing to oil free compressor. In addition simple design of test compressor removes presence of nose generated by synchronising and high ratio driving gears which highly affect overall compressor noise. Therefore noise generated by test compressor will be mainly due to gas pulsations.

Compressor design parameters			Main	Gate
		Number Of Lobes	4	5
Centre distance	71 [mm]	Outer Diameter	102 [mm]	80 [mm]
Rotor length	158 [mm]	Pitch Diameter	63 [mm]	79 [mm]
Wrap angle	300 [deg]	Inner Diameter	62 [mm]	40 [mm]
Pressure range	3-12 [bar]	Speed range	2000-6500 [rpm]	

Table 1. Screw compressor design parameters

Test compressors are positioned in the test rig built at City University London. The compressor testing range has been defined to cover compressor speed and pressure range as it is shown in Table 2. Testing range covers 40 measuring points (MP) which requires significant amount of time to be spent for experimental and numerical investigation.

	Pressure[bar]							
Speed [rpm]	5	6	7	8	9	10	11	12
2000				MP				
3000				MP				
4000	MP	MP	MP	MP	MP	MP	MP	MP
5000				MP				
6000				MP				

Table 2. Screw compressor testing range

Number of measuring points can be reduced to smaller number which will be enough to describe compressor behavior under different conditions. So, the number of measuring points is lowered to only 12 which still provide enough information regarding influences of the design changes upon gas pulsations. Measuring points cover a range of compressor speeds from 2000 to 6000 [rpm] at a discharge pressure of 8 [bar]. Another set of points covers discharge pressures from 5 to 12 [bar] at the same speed of 4000 [rpm].

Experiment has covered measurement of following parameters. Discharge chamber pressure has been measured by use of a Piezo-electric pressure sensor Endevco model 8530C to obtain pressure transfer function. Sound pressure level (SPL) around of testing compressor has been measured to evaluate changes in pressure transfer function upon overall compressor noise. For this purpose sound pressure level indicators SJK Scientific Ltd – Integrating Averaging Sound Level Meter HML 323 have been used. Measurements of pressure, temperature, driving torque, air flow and compressor speed also has been done to estimate compressor performance.

4.2. Compressor discharge port modification

To reduce amplitudes of gas pulsations modification of the discharge port is implemented here. The port has to be modified in that way that reduces sudden flow between working and the discharge chamber at the beginning of the discharge process when the pressure difference between them is highest. That flow is governed by pressure difference and size of the port area according to equation (1). As built in volume ratio should not be changed that means that the pressure difference must be the same when discharge starts for modified ports as well. On the other side the size of the discharge port can be changed to reduce sudden flow. The conventional discharge port is designed to have largest possible opening for the arbitrary rotor position to reduce flow loses. This is achieved by the port shape which follows rotor trailing edges. Such approach generates area transfer function with high starting gradient as shown by light line in Figure 4.a. In that case the largest possible port area is open when the pressure difference is largest.

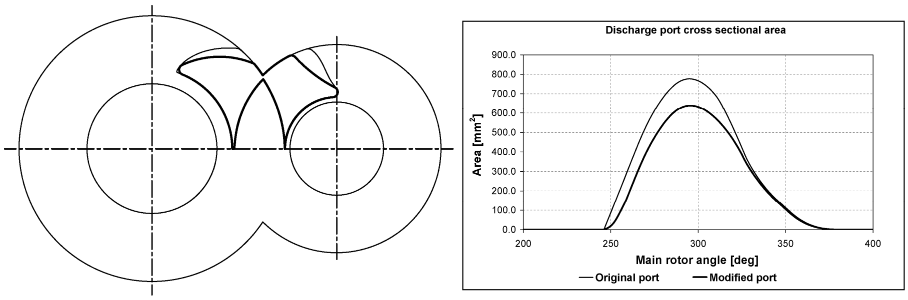

a) b)

Figure 4 Shape and cross sectional area of two different discharge ports

To avoid that new shape of the port is proposed as shown by bold line in Figure 4.a. It is noticeable that only port opening curves have been changed. This is to change starting gradient of the area transfer function. The port is design to preserve the same built in volume ratio. This is achieved by designing new port to share some parts of the opening curves with original port. By this mean both port will open at the same rotor position.

Opening curves are in this case fairly simple consisting of three arcs comparing to complex shape of the old ones. Bold line shown in Figure 4.b represents area transfer function of the modified port while light line represents original port. It is noticeable that the starting gradient has been changed which was the intention.

Change in shape of the port results with reduction in size of the port area. The difference arises at the beginning of the opening and rich highest difference when the port is most opened. Towards the end difference is reducing and finally disappears when leading edges of the following rotor lobes completely covers opening curves. Such reduction can cause some flow loses.

4.3. Prediction and verification of results

Pressure transfer function in the discharge chamber predicted by thermodynamic model of the discharge process is shown by bold lines in Figure 6 and Figure 7. Figure 6 shows predicted pressure transfer function of the original discharge port shape. In Figure 7 is shown prediction for the modified port shape. Used thermodynamic model was able to account for changes of the discharge port shape. Analyzing predicted results it is obvious that modified discharge port produces lower level of gas pulsations.

To verify model and to confirm predicted results experimental investigation has been carried out for two different shapes of the discharge port. Object of first experiment was compressor with original shape of the port. Pressure transfer function for original port obtained by experiment is shown by light line in Figure 6. The results show that the prediction of gas pulsations in the discharge ports is in line for the amplitudes which correspond to compressor fundamental frequency. Higher harmonics this model is not able to predict. The thermodynamic model described here neglects compressor piping system, oil separators, etc. Reflection waves which occur in these components are the main reason why experimental data differ from predicted results in some parts of the cycle. It has been previously reported that one dimensional model is accurate for a very narrow frequency range [5]. This model confirms that statement.

However, model predicts very well amplitude which corresponds to the compressor fundamental frequency across whole compressor pressure and speed range. This amplitude is influenced more by the process which arises in the discharge port then by wave reflection. Therefore, the model is suitable for investigation influence of the discharge port shape upon pulsations amplitudes on compressor fundamental frequency.

To verify predicted results for the modified shape of the discharge port compressor geometry had to be changed is shown in Figure 5. Metal inserts form shape of the new port. Those inserts also cover old opening curves on both sides of the port. Old opening curves are illustrated in Figure 5 by two lines on metal inserts. After modification new set of measurement has been carried out in order to confirm predicted gas pulsations. Experimental results shown by light line in Figure 7 follows reasonable well prediction.

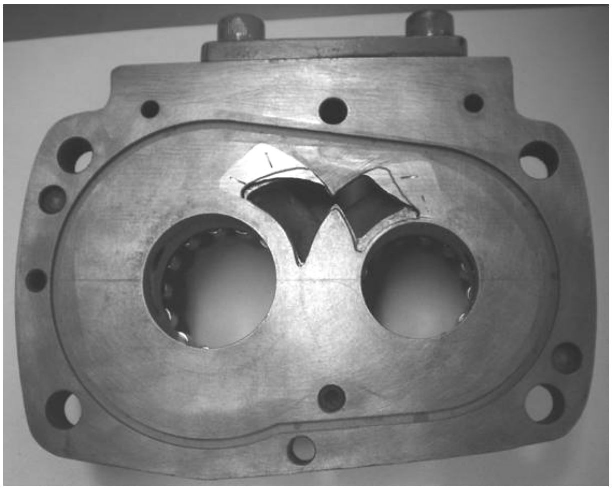

Figure 5 Modified shape of the discharge port

Shown in Figure 8 are pressure transfer functions in the discharge chamber for original and modified discharge ports obtained by experiment. Pressure transfer functions for original and modified port are presented by light and bold line respectively. It can be seen that reduction of gas pulsations amplitudes is achieved across the whole range of the working conditions. Sound pressure level generated by gas pulsations in the discharge chamber is reduced, according to Figure 9, in range of 3 to 5 [dB].

Achieved reduction in gas pulsation is transferred further to overall noise reduction. Figure 9 shows that noise in compressor environment is attenuated for about 3[dB] at compressor speed of 4000[rpm] for whole pressure range. Noise reduction is noticeable also across the compressor speed range as it is shown in Figure 9. For outlet pressure of 8[bar] the noise reduction goes from 2[dB] at lowest speed up to 5[dB] at compressor maximum speed.

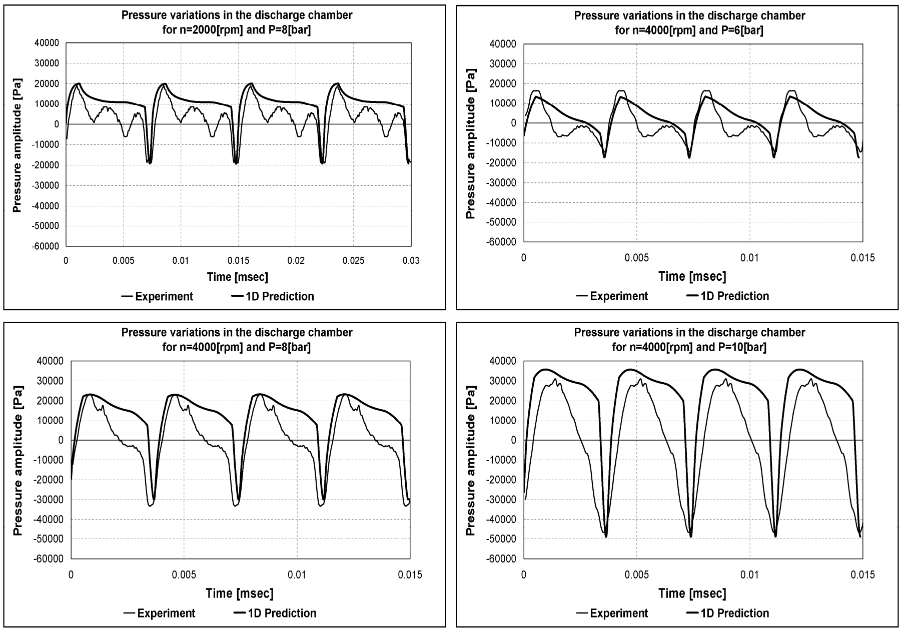

Figure 6 Comparison of experimental data and results of thermodynamic simulation for original discharge port

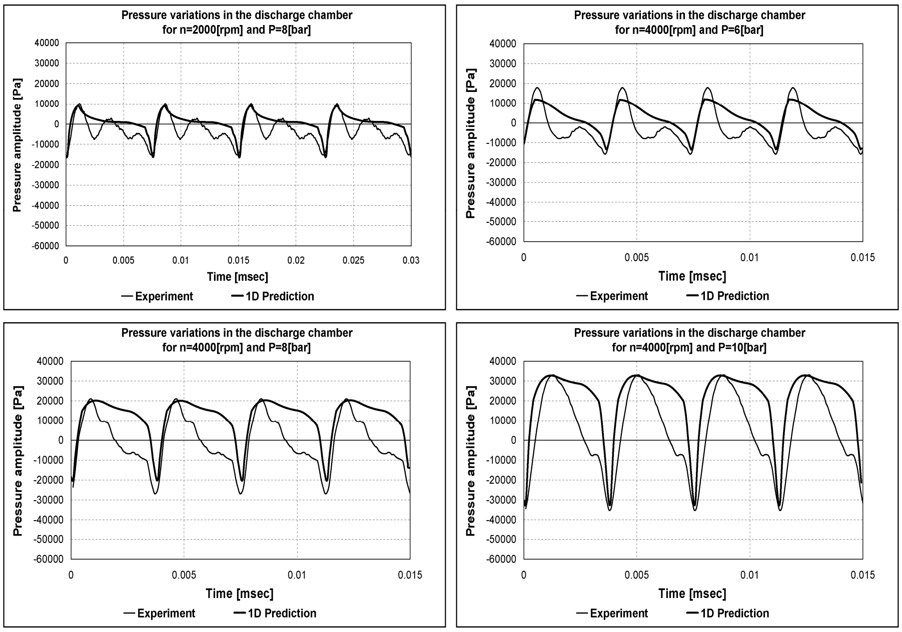

Figure 7 Comparison of experimental data and results of thermodynamic simulation for modified discharge port

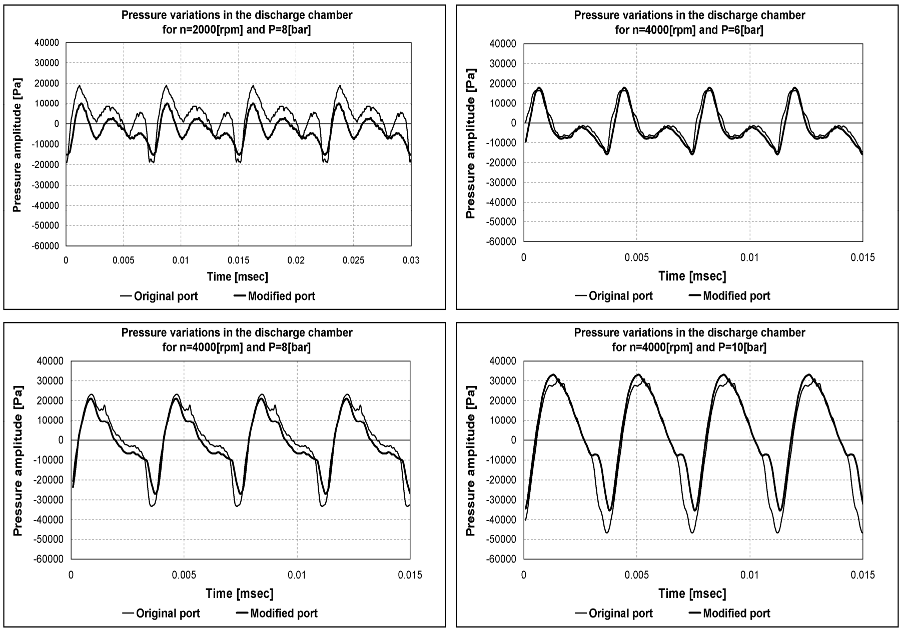

Figure 8 Comparison of experimental data for original and modified discharge ports

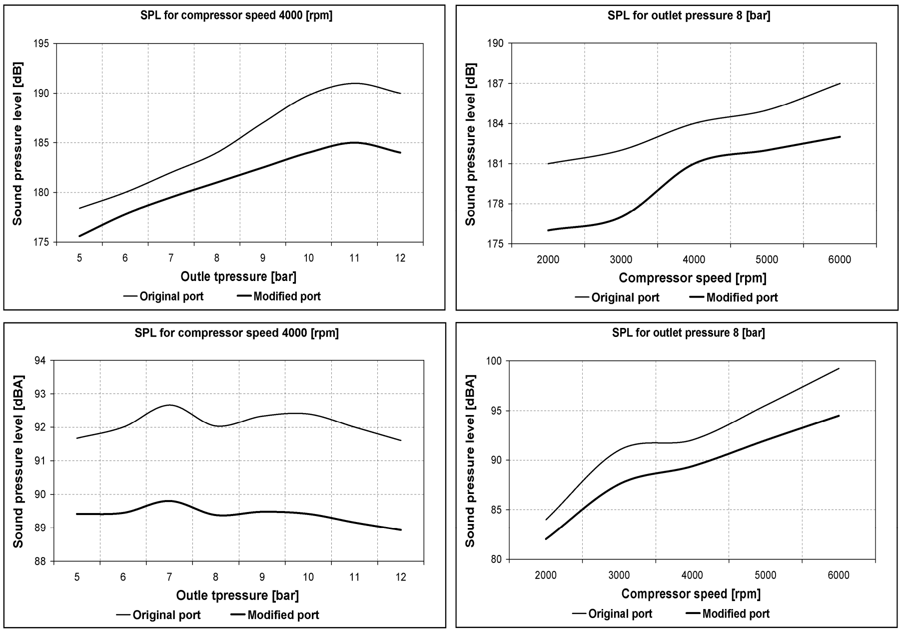

Figure 9 Comparison of calculated SPL inside the discharge chamber and measured SPL around compressor for original and modified discharge ports

5. CONCLUSION

Two basic influential parameters upon gas pulsations are determined here, pressure difference and discharge port area. A simplified model was applied to calculate the pressure transfer function in screw compressor discharge chamber in order to evaluate the influence of the discharge port size and shape upon gas pulsations. The results obtained with it were compared with test results on a compressor with two different port shapes. These agreed well and confirm that the shape and size of the discharge port determine level of gas pulsations in the discharge chamber. It follows that gas pulsations in screw compressor discharge port and consequently the generated noise can be reduced by appropriate size and shape of the discharge port.

REFERENCE LIST

1. **Erol H & Ahmet G, 2000:** The noise and vibration characteristics of reciprocating compressor: Effects of size and profile of discharge port, In The 2000 International Compressor Engineering Conference at Perdue, pp. 677-683

2. **Fujiwara A & Sakurai N, 1986:** Experimental analysis of Screw Compressor Noise and Vibration, In The 1986 International Compressor Engineering Conference at Perdue

3. **Gavric L & Badie-Cassagnet A, 2000:** Mesurement of fas pulsations in discharge and suction lines of refrigerant compressors, In The 2000 International Compressor Engineering Conference at Perdue, pp. 627-634

4. **Huagen W, Ziwen X, Xueyuan P, Pengcheng S 2004:** Simulation of discharge pressure pulsation within twin screw compressors, IMechE 2004, School of Energy and Power Engineering, Xi'an Jiaotong University, Xi'an, P. R. China

5. **Koai K L & Soedel W, 1990:** Gas pulsations in twin screw compressors – Part I: Determination of port flow and interpretation of periodic volume source, In The 1990 International Compressor Engineering Conference at Perdue, pp. 369-377

6. **Koai K L & Soedel W, 1990:** Gas pulsations in twin screw compressors – Part II: Dynamics of discharge system and its interaction with port flow, In The 1990 International Compressor Engineering Conference at Perdue, pp. 378-387

7. **Kovacevic A, 2007**: 1D-3D model, International Conference on Compressors and their Systems 2007, London, UK

8. **Mujic E, Kovacevic A, Stosic N, Smith I K, 2005:** Analysis and measurement of discharge port influence upon screw compressor noise, TMT 2005, Antalya, Turkey

9. **Sangfors B, 1999:** Computer simulation of gas-flow noise from twin-screw compressors, In International Conference on Compressor and Their Systems, 13-15, London, pp.707-716

10. **Stosic N, Hanjalic K :** Development and Optimization of Screw Machines With a Simulation Model – Part II: Thermodynamic Performance Simulation and Design Optimization, Journal of Engineering Design, Vol.8, 389

11. **Tanttari J, 2000:** On Twin-Screw Compressor Gas Pulsation Noise, The 29th International Congress and Exhibition on Noise Control Engineering, Nice, France